

## Spectroelectrochemical sensing based on multimode selectivity simultaneously achievable in a single device

### 14. Enhancing sensitivity of a metal complex ion by ligand exchange

Tanya Shtoyko<sup>a</sup>, John N. Richardson<sup>b</sup>, Carl J. Seliskar<sup>a</sup>, William R. Heineman<sup>a,\*</sup>

<sup>a</sup> Department of Chemistry, University of Cincinnati, P.O. Box 210172, Cincinnati, OH 45221-0172, USA

<sup>b</sup> Department of Chemistry, Shippensburg University, 1871 Old Main Drive, Shippensburg, PA 17257, USA

Received 16 July 2004; received in revised form 16 November 2004; accepted 20 November 2004

Available online 5 January 2005

#### Abstract

Enhancement of the sensitivity of a spectroelectrochemical sensor by ligand exchange within the sensing film during spectroelectrochemical modulation is demonstrated in this paper. This concept is illustrated with a sensor for  $\text{Cu}(\text{en})_2^{2+}$ , where en = ethylenediamine, in aqueous solution. A ligand exchange reaction increases the difference in the molar absorptivities of the two complex ions involved in spectroelectrochemical modulation, thus giving a larger optical response. The spectroelectrochemical sensor consists of a cation-selective Nafion-SiO<sub>2</sub> composite film spin-coated onto an indium tin oxide (ITO) glass optically transparent electrode (OTE). The film was loaded with 2,9-dimethyl-1,10-phenanthroline (neocuproine, or nc) for the ligand exchange reaction. Reduction of  $\text{Cu}(\text{en})_2^{2+}$  at the OTE is accompanied by ligand exchange with nc to form  $\text{Cu}(\text{nc})_2^{1+}$ , which has a molar absorptivity of  $7950 \text{ M}^{-1} \text{ cm}^{-1}$  at  $\lambda_{\text{max}} = 454 \text{ nm}$ . Detection within the sensing film using attenuated total reflectance (ATR) at 454 nm during modulation was accomplished by potential cycling between 0.8 and  $-0.9 \text{ V}$  versus Ag/AgCl. The effects of nc concentration in the film and potential scan rate on the absorbance–time profile for spectroelectrochemical modulation were studied. The calibration curve for  $\text{Cu}(\text{en})_2^{2+}$  was linear within the range of  $5 \times 10^{-6} \text{ M}$  to  $1 \times 10^{-3} \text{ M}$ .

© 2004 Elsevier Ltd. All rights reserved.

**Keywords:** Nafion-SiO<sub>2</sub> composite film; Spectroelectrochemical modulation; Ethylenediamine; Optically transparent electrode; Neocuproine

#### 1. Introduction

A new type of sensor exhibiting three modes of selectivity (chemical partitioning into a selective thin film, electrochemistry and spectroscopy) has been under development in our laboratory for some time [1–14]. Detection of analyte occurs by observing changes in an optical signal associated with spectroelectrochemical modulation of the analyte after it partitions into the selective film, which is coated onto an optically transparent electrode (OTE). The sensor has been previously demonstrated with a series of metal ion complexes such as  $\text{Fe}(\text{CN})_6^{3-/4-}$  [2,10,14],  $[\text{Re}(\text{dmpe})_3]^+$  [7,8],  $\text{Ru}(\text{bipy})_3^{2+}$  [9], and a cationic organic compound (methyl

viologen dication [12]), all of which exhibited both electrochemical reversibility and a substantial difference in molar absorptivity during spectroelectrochemical modulation. Both of these features are advantageous to development of a sensitive spectroelectrochemical sensor.

New materials for films that possess properties suited to construction of spectroelectrochemical sensors, such as ion-exchangeability, nanoscale porosity, high optical transparency, variable thickness, and physicochemical stability have been developed [13,15,16]. These materials are essential to the functioning of this spectroelectrochemical sensor. One series of materials is based on polymer blending in a host of glutaraldehyde cross-linked poly(vinyl alcohol) [13,16]. Chemically-selective dopants in this host demonstrate property-selective separations of chemicals from mixtures [13,16]. A second series consists of polyelectrolyte-

\* Corresponding author. Tel.: +1 513 556 9210; fax: +1 513 556 9239.  
E-mail address: [heinemwr@email.uc.edu](mailto:heinemwr@email.uc.edu) (W.R. Heineman).

containing silica composites prepared by sol–gel processing [15].

More recently, we have begun exploring strategies whereby analytes that do not exhibit ideal properties may still be detected by the spectroelectrochemical sensor. The possibility of using the spectroelectrochemical concept to detect an analyte that itself does not exhibit a measurable optical change associated with its electrolysis was recently demonstrated [11]. This sensor was based on a mediated electrode reaction in which a non-absorbing analyte (ascorbate) was detected indirectly by its effect on the optical signal resulting from the spectroelectrochemical modulation of the mediator ( $\text{Ru}(\text{bipy})_3^{2+}$ ), which had been trapped in a cation-selective Nafion-SiO<sub>2</sub> composite film [11].

A second example is the determination of  $\text{Fe}^{2+}$  in aqueous solution [17]. Both  $\text{Fe}^{2+}$  and  $\text{Fe}^{3+}$  ions are only weakly absorbing in aqueous solution and thus are not directly amenable to detection by spectroelectrochemical modulation. To overcome this problem, the ligand 4,4'-bipyridyl (bipy) was loaded into a Nafion film on the OTE.  $\text{Fe}^{2+}$  partitioned from the aqueous sample into the Nafion film where it reacted with bipy to form the intense chromophore  $\text{Fe}(\text{bipy})_3^{2+}$  [17]. Spectroelectrochemical modulation between the intensely colored  $\text{Fe}(\text{bipy})_3^{2+}$  and colorless  $\text{Fe}(\text{bipy})_3^{3+}$  gave a substantially increased sensitivity because of the large difference in molar absorptivity ( $\Delta\varepsilon$ ) between the two species [17].

The objective of this research was to demonstrate another mechanism for sensing that enhances detection by increasing  $\Delta\varepsilon$  between the species involved in spectroelectrochemical modulation. In this mechanism a metal complex analyte undergoes a reversible ligand exchange reaction with another ligand in the sensing film as part of the spectroelectrochemical modulation process. The exchange ligand is chosen to increase  $\Delta\varepsilon$  and is immobilized in the sensing film prior to exposure to the analyte. We used  $\text{Cu}(\text{en})_2^{2+}$ , where en = ethylenediamine, as a representative analyte and 2,9-dimethyl-1,10-phenanthroline (neocuproine, or nc) as the exchange ligand trapped in a selective Nafion-SiO<sub>2</sub> film. The sequence of events that occurs in the sensor is shown schematically in Fig. 1.  $\text{Cu}(\text{en})_2^{2+}$  first partitions into the sensing film where it can be controlled electrochemically and monitored optically by the evanescent wave component at the reflection points of the optical beam. Weakly absorbing  $\text{Cu}(\text{en})_2^{2+}$  is reduced by one electron; this process is accompanied by ligand exchange with nc to form the intensely absorbing  $\text{Cu}(\text{nc})_2^{1+}$ . The large  $\Delta\varepsilon$  in these two species gives rise to a large change in absorbance,  $\Delta A$ , which is used to quantify the analyte,  $\text{Cu}(\text{en})_2^{2+}$ .

## 2. Experimental

### 2.1. Chemicals and materials

All chemicals were used as received without further purification: tetraethoxysilane (TEOS), Nafion (5% solution in

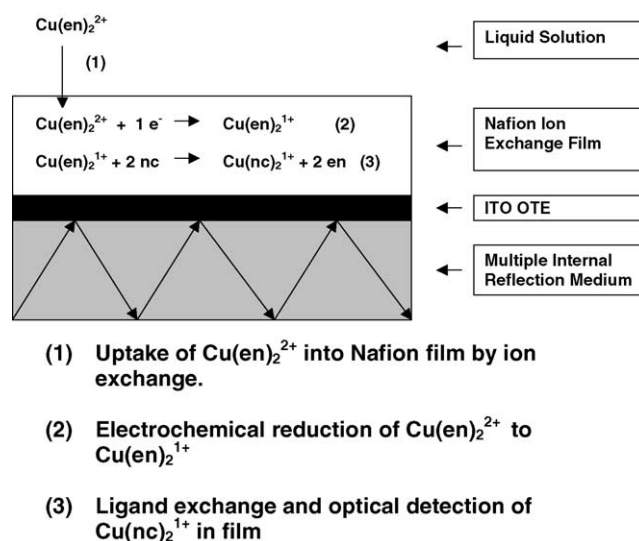


Fig. 1. Diagram of  $\text{Cu}(\text{en})_2^{2+}$  sensing using nc.

lower aliphatic alcohols and water), and neocuproine (98%) by Aldrich; ethylenediamine from Aldrich; hydrochloric acid (Reagent A.C.S.), ethanol and potassium nitrite from Fisher Scientific; and cupric sulfate from Mallinckrodt.

Copper (II) sulfate solutions were made by dissolving the appropriate amount in 0.1 M  $\text{KNO}_3$ . The appropriate amount of ethylenediamine was added to copper sulfate solutions to make the solution 0.1 % en. A 0.2 M neocuproine solution was made by dissolving the appropriate amount in ethanol. The resulting neocuproine solution was dissolved in water to make a 1:3 (v/v) nc solution. Indium tin oxide (ITO)-coated glass (11–50  $\Omega/\text{sq}$ , 150 nm thick ITO layer over tin float glass) was supplied by Thin Film Devices. A 1-PM101DT-R485 Photo-Resist-Spinner, manufactured by Headway Research Inc., was used for spin-coating films onto the ITO electrode surfaces.

### 2.2. Nafion-SiO<sub>2</sub> selective film preparation

The preparation of the Nafion-SiO<sub>2</sub> composite film was performed as previously described [15]. Briefly, 4 mL of deionized water, 2 mL of TEOS, and 0.1 mL of 0.1 M HCl were mixed for 3 h until a single-phase sol resulted. The sol was blended with a solution of Nafion in a ratio of 1:3 (v/v). 300  $\mu\text{L}$  of the mixture were immediately spin-coated onto ITO-glass substrates at a spin rate of 3000 rpm for 30 s. The slides were cured in air at room temperature for at least a day. The slides were then hydrated by soaking in supporting electrolyte solution for at least 12 h. Unless otherwise noted, the slides were immersed ( $\sim 1$  h) in 0.04 M neocuproine ethanol–water solution (1:3 v/v) for ligand uptake.

Film thickness was estimated by the optical interference fringe method [18] and ellipsometry (Woollam) and ranged from 300 to 380 nm.

### 2.3. Thin layer spectroelectrochemistry

Thin layer spectroelectrochemistry employing an optically transparent thin layer electrode (OTTLE) [19] was used to initially characterize the spectroelectrochemical properties of the different complex ions. An ITO-glass slide was used as an optically transparent electrode, and the OTTLE was constructed using standard literature procedures [19,20]. The reference electrode used in all electrochemical experiments was Ag/AgCl/3M NaCl.

### 2.4. Attenuated total internal reflection (ATR) measurements

The instrument for spectroelectrochemical modulation has been previously described [2]. ATR spectroelectrochemical measurements were performed using a simple Delrin plastic cell, also described previously [2]. The potential and corresponding ATR signal were digitized and stored on a personal computer. Data records were manipulated and analyzed using spreadsheet programs. The angle of incidence of light into the coupling prism and the alignment of the cell were adjusted to maximize the ATR throughput, as determined by measuring the intensity of decoupled light. Sensor absorbance values were obtained by recording the light intensity through the prism-coupled slide when exposed to pure supporting electrolyte ( $I_0$ ) and the intensity after being exposed to an analyte solution ( $I$ ). Sensor absorbance in the multiple reflection arrangement was defined as  $A = \log(I_0/I)$ .

## 3. Results and discussion

The main goal of this research was to demonstrate ligand exchange in a metal complex analyte during spectroelectrochemical sensing to enhance its detection.  $\text{Cu}(\text{en})_2^{2+}$  served as the analyte and nc as the exchange ligand. Since the analyte is cationic, a Nafion-SiO<sub>2</sub> [15] film was used as a cation-exchange selective layer into which  $\text{Cu}(\text{en})_2^{2+}$  was pre-concentrated for sensing. Nafion also served to trap the hydrophobic exchange ligand, nc, because of its hydrophobic domains.

### 3.1. Spectral characterization

Spectral characteristics of the various copper species involved are shown in Table 1. The near infrared absorbance of  $\text{Cu}^{2+}$  results from a  $d-d$  transition. For Cu complexes the wavelength of maximum absorbance ( $\lambda_{\text{max}}$ ) and  $\epsilon$  depend

on the coordinating ligand and in aqueous solution are pH-dependent since  $\text{OH}^-$  and  $\text{H}_2\text{O}$  are available ligands. A spectrum of  $\text{Cu}^{2+}$  measured in copper sulfate solution gave  $\epsilon$  of  $12 \text{ M}^{-1} \text{ cm}^{-1}$  at  $\lambda_{\text{max}} = 810 \text{ nm}$ . If en is added to an aqueous solution of  $\text{Cu}^{2+}$ , the very stable complex  $\text{Cu}(\text{en})_2^{2+}$  forms ( $\log \beta_2 = 19.6$ ) [21] in the pH range from 11.2 to 6.5. Visible spectra of  $\text{Cu}(\text{en})_2^{2+}$  at pH values between 6 and 11.2 show an absorption peak at 547 nm and indicate that  $\text{Cu}(\text{en})_2^{2+}$  is stable over that range of pH. At  $\text{pH} < 6$ ,  $\text{Cu}(\text{en})_2^{2+}$  decomposes due to en dissociation via protonation (spectra not shown). Spectra of  $\text{Cu}(\text{en})_2^{2+}$  in 0.1 M  $\text{KNO}_3$ , which is the medium used for all of the sensing experiments, gave  $\epsilon = 75 \text{ M}^{-1} \text{ cm}^{-1}$  at  $\lambda_{\text{max}} = 547 \text{ nm}$ . If the pH of the solution is made basic ( $\sim 11.2$ ), cupric hydroxide does not precipitate, and hydroxide complexes of copper do not form because  $\text{Cu}(\text{en})_2^{2+}$  is much more stable than these species [21].

$\text{Cu}^{2+}$  in aqueous solution slowly forms a square planar complex with neocuproine  $\text{Cu}(\text{nc})_2^{2+}$  [24] ( $\log \beta_2 = 11.4$ ) [21], which is not a preferred configuration.  $\text{Cu}(\text{nc})_2^{2+}$  is a stable orange complex with  $\epsilon = 3550 \text{ M}^{-1} \text{ cm}^{-1}$  at  $\lambda_{\text{max}} = 454 \text{ nm}$ . However, if  $\text{Cu}^{2+}$  is reduced to  $\text{Cu}^+$  in the presence of nc, the more stable orange tetrahedral complex  $\text{Cu}(\text{nc})_2^+$  ( $\log \beta_2 = 19.1$ ) [21] shown below forms [22]. This complex ion also has a  $\lambda_{\text{max}}$  at 454 nm [22], but a much larger  $\epsilon$  of  $7950 \text{ M}^{-1} \text{ cm}^{-1}$  because the electronic transition in question involves significant ligand molecular orbital character.  $\text{Cu}(\text{nc})_2^+$  is stable for long periods of time over a wide pH range [22,23]. However, the absorbance of a solution of  $\text{Cu}(\text{nc})_2^+$  decreases dramatically in the presence of free  $\text{Cu}^{2+}$  due to formation of a mixed ligand complex when there is not an excess of nc in the solution [21].

The formation constants and spectral properties of the two complexes of copper in their different oxidation state supports the following scheme upon which the sensor is based. Reduction of  $\text{Cu}(\text{en})_2^{2+}$  to  $\text{Cu}(\text{en})_2^+$  ( $\log \beta_2 = 11.2$ ) [21] in excess nc results in ligand substitution to form the more stable  $\text{Cu}(\text{nc})_2^+$  ( $\log \beta_2 = 19.1$ ) [21]; this reaction is accompanied by a large increase in absorbance at 454 nm. Oxidation of  $\text{Cu}(\text{nc})_2^+$  to  $\text{Cu}(\text{nc})_2^{2+}$  ( $\log \beta_2 = 11.4$ ) [21] in the presence of excess en should result in ligand exchange to reform the more stable  $\text{Cu}(\text{en})_2^{2+}$  ( $\log \beta_2 = 19.6$ ) [21], and the absorbance decreases to its original value. Since  $\epsilon$  for  $\text{Cu}(\text{nc})_2^+$  is about 800 times larger than  $\epsilon$  for  $\text{Cu}(\text{en})_2^{2+}$  (Table 1), the spectroelectrochemical modulation of  $\text{Cu}(\text{en})_2^{2+}$  in excess nc should be quite sensitive.

This chemistry as it applies to the spectroelectrochemical sensor is depicted in Fig. 1.  $\text{Cu}(\text{en})_2^{2+}$  partitions from the sample solution into the film of Nafion-SiO<sub>2</sub>, which also contains the exchange ligand nc. Reduction of  $\text{Cu}(\text{en})_2^{2+}$

Table 1  
Formation constants and molar extinction coefficients for copper complexes

| Ligand               | $\text{Cu}^+$  | $\text{Cu}^{2+}$  |
|----------------------|--|---|
| $\text{H}_2\text{O}$ | $\epsilon = 9 \text{ M}^{-1} \text{ cm}^{-1}$ (790 nm)   | $\epsilon = 12 \text{ M}^{-1} \text{ cm}^{-1}$ (810 nm)   |
| nc                   | $\log \beta_2 = 19.1$ , $\epsilon = 7950 \text{ M}^{-1} \text{ cm}^{-1}$ (454 nm), tetrahedral | $\log \beta_2 = 11.4$ , $\epsilon = 3550 \text{ M}^{-1} \text{ cm}^{-1}$ (454 nm) square planer |
| en                   | $\log \beta_2 = 11.2$ , $\epsilon = 39 \text{ M}^{-1} \text{ cm}^{-1}$ (547 nm)                | $\log \beta_2 = 19.6$ , $\epsilon = 75 \text{ M}^{-1} \text{ cm}^{-1}$ (547 nm)                 |

results in formation of the more stable, strongly absorbing  $\text{Cu}(\text{nc})_2^{1+}$ , which gives rise to a large increase in absorbance. Subsequent oxidation of this complex ion forms the original  $\text{Cu}(\text{en})_2^{2+}$ , resulting in a concomitant decrease in absorbance, thus leading to optical modulation in response to electrochemical cycling of the potential.

### 3.2. Cyclic voltammetry and spectroelectrochemistry

Previous voltammetric studies indicate that the electrochemical behavior of  $\text{Cu}^{2+}$  in water strongly depends on the presence (or absence) of certain ligands [21,24–27]. In the absence of a strongly complexing ligand,  $\text{Cu}^{2+}$  reduces to

$\text{Cu}^0$ , which deposits on the electrode. Any intermediate  $\text{Cu}^+$  ion formed disproportionates to form the more stable  $\text{Cu}^{2+}$  and  $\text{Cu}^0$  species [28]. However,  $\text{Cu}^+$  can be trapped by allowing it to react with a strong complex forming ligand such as neocuproine [21]. This process is evidenced by the shift in the standard potential of the  $\text{Cu}^{2+}/\text{Cu}^+$  couple to more positive potentials after preferential complexation of  $\text{Cu}^+$ .

The electrochemistry and spectroelectrochemistry of  $\text{Cu}^{2+}$  at a bare ITO OTE were investigated using cyclic voltammetry. Fig. 2A shows cyclic voltammograms of  $\text{Cu}^{2+}$  in 0.1 M  $\text{KNO}_3$  at pH 7.3 (curve 2) and of supporting electrolyte (curve 1) within the potential window of 1.2 to  $-0.5$  V. The pH of 7.3 is the natural value for the solution, and no attempt was made

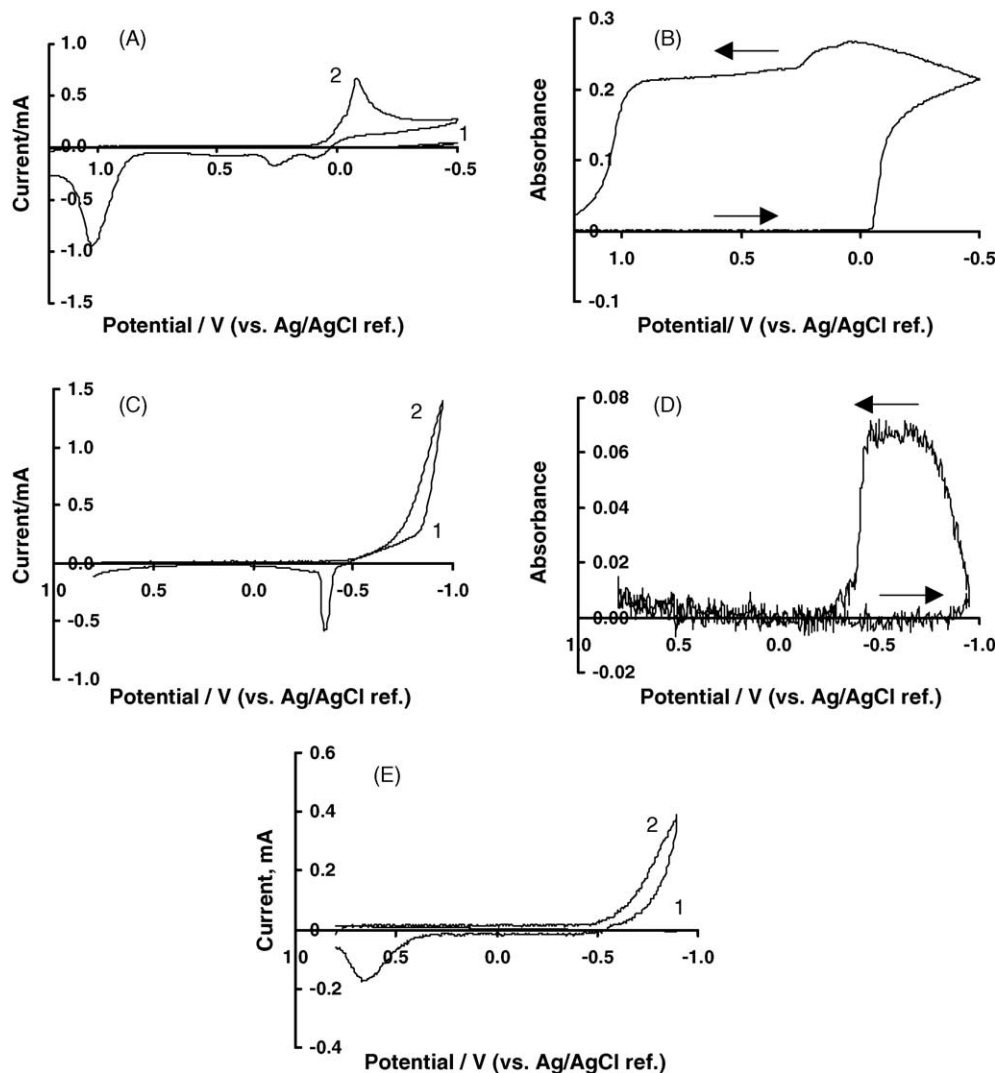


Fig. 2. (A) Cyclic voltammograms recorded at a bare ITO OTE in (1) 0.1 M  $\text{KNO}_3$  and (2)  $1 \times 10^{-3}$  M  $\text{CuSO}_4$  in 0.1 M  $\text{KNO}_3$ . Each voltammogram was recorded by cycling the potential in the range from 1.2 V to  $-0.5$  V (vs. Ag/AgCl ref.) at a potential scan rate of 5 mV/s. (B) ATR sensor absorbance measured at 400 nm taken concurrently with the cyclic voltammogram shown in (A). (C) Cyclic voltammograms recorded at a bare ITO OTE of solutions containing (1)  $4 \times 10^{-3}$  M en and 0.1 M  $\text{KNO}_3$  and (2)  $1 \times 10^{-3}$  M  $\text{CuSO}_4$  with  $4 \times 10^{-3}$  M en in 0.1 M  $\text{KNO}_3$ . Each voltammogram was recorded by cycling the potential between 0.9 V and  $-1.2$  V ( $\nu = 5$  mV/s, E vs. Ag/AgCl ref.). (D) Sensor absorbance measured at 400 nm taken concurrently with the cyclic voltammogram shown in (C). (E) Cyclic voltammograms recorded at a bare ITO OTE in (1)  $4 \times 10^{-3}$  M nc,  $4 \times 10^{-3}$  M en and 0.1 M  $\text{KNO}_3$  in a 1:3 (v/v) solution of ethanol in water; (2)  $1 \times 10^{-3}$  M  $\text{CuSO}_4$ ,  $4 \times 10^{-3}$  M en,  $4 \times 10^{-3}$  M nc, and 0.1 M  $\text{KNO}_3$  in a 1:3 (v/v) solution of ethanol in water. The voltammograms were recorded by cycling the potential in the range from 0.8 V to  $-0.9$  V at 5 mV/s, (E vs. Ag/AgCl ref.).

to adjust or control it. The associated optical response (transmission) for the  $\text{Cu}^{2+}$  voltammogram is shown in Fig. 2B. The voltammogram has a single distinctive reduction peak for  $\text{Cu}^{2+}$  with a small shoulder on the forward scan and multiple oxidation peaks on the reverse scan. The reduction wave is associated with a sharp increase in absorbance. We attribute this to deposition of Cu on the OTE because it is essentially wavelength independent (i.e., behaves like a neutral density filter) and is considerably larger than can be attributed to the formation of  $\text{Cu}^+$  based on values of  $\epsilon$  in Table 1. This behavior is consistent with previous work showing that  $\text{Cu}^{2+}$  reduction in water is not by one electron to  $\text{Cu}^+$ , but two electrons to  $\text{Cu}^0$ . As reported previously [29], the first anodic peak (ca. 0.1 V in this case) was attributed to formation of a surface  $\text{Cu}_2\text{O}$  layer. The second peak (at 0.3 V in our case) was attributed to oxidation of bulk copper to  $\text{Cu}_2\text{O}$  [29]. The concurrent decrease in absorbance during copper oxidation to  $\text{Cu}_2\text{O}$  was reported before [29] and is due to electrochromism of copper oxide thin films. The dominant stripping peak occurring at 1.35 V (versus Ag/AgCl) corresponds to the stripping of  $\text{Cu}_2\text{O}$  from the ITO surface. All of the oxidation waves are accompanied by a decrease in absorbance as expected for electrochromism and the removal of Cu from the OTE. It is apparent that spectroelectrochemistry is very sensitive to the formation of solid Cu and its oxides on the electrode surface. In fact, we have recently reported a sensor for Cu based on the optical changes that accompany its deposition and stripping on a bare ITO surface [30].

The addition of excess en into solution converts aqueous  $\text{Cu}^{2+}$  to  $\text{Cu}(\text{en})_2^{2+}$  and raises the pH to 11.2 by hydrolysis of excess ligand. Cyclic voltammetry (Fig. 2C) and the associated optical response (Fig. 2D) show the reduction of  $\text{Cu}(\text{en})_2^{2+}$  to be energetically more difficult than that of  $\text{Cu}^{2+}$  as evidenced by the negative shift in the reduction wave ( $E_{\text{pc}} < -1.0$  V, not shown in Fig. 2C due to onset of hydrogen reduction), as expected for the formation of the stable complex. Reduction of  $\text{Cu}(\text{en})_2^{2+}$  is accompanied by a sharp increase in absorbance, which is also due to reduction to  $\text{Cu}^0$  as evidenced by the magnitude of the change.  $\text{Cu}^0$  oxidizes more easily (sharp stripping peak at  $E_{\text{pa}} = -0.3$  V) in the presence of en because stable  $\text{Cu}(\text{en})_2^{2+}$  forms. Stripping of  $\text{Cu}^0$  returns the absorbance to its original baseline. Thus, reduction of  $\text{Cu}(\text{en})_2^{2+}$  is to  $\text{Cu}^0$ , with no apparent formation of  $\text{Cu}(\text{en})_2^{1+}$ .

The electrochemistry is changed significantly by adding nc to the solution containing  $\text{Cu}(\text{en})_2^{2+}$ . During  $\text{Cu}(\text{en})_2^{2+}$  reduction with nc excess in the solution, preferential complexation of  $\text{Cu}^+$  with nc shifts the reduction potential to a less negative potential (Fig. 2E).  $\text{Cu}(\text{nc})_2^{1+}$  complex formation prevents further copper reduction to  $\text{Cu}^0$ . No evidence of deposition or stripping of  $\text{Cu}^0$  on the ITO OTE was seen in the voltammogram or optically at 400 nm (not shown in Fig. 2). The anodic peak in Fig. 2E corresponds to oxidation of  $\text{Cu}(\text{nc})_2^{1+}$  accompanied by ligand exchange with en to reform the more stable  $\text{Cu}(\text{en})_2^{2+}$ . As

evidenced by the large separation in cathodic and anodic peak potentials, this is not an electrochemically reversible process.

Thin layer spectroelectrochemistry at an OTTLE was used to confirm that  $\text{Cu}(\text{en})_2^{2+}$  can be electrochemically cycled between  $\text{Cu}(\text{en})_2^{2+}$  and  $\text{Cu}(\text{nc})_2^{1+}$  without formation of  $\text{Cu}^0$  in the presence of excess nc. The experiment consisted of loading the cell with a solution of  $\text{Cu}(\text{en})_2^{2+}$  containing excess nc, applying an initial positive potential, and scanning the potential negatively and then positively again while recording spectra simultaneously to characterize the formed species. Fig. 3 shows transmission spectra of the 7.5 mM  $\text{Cu}(\text{en})_2^{2+}$  solution with excess nc as taken during the reduction/oxidation process. Spectrum (a) was recorded throughout the slow potential scan from 0.8 V to  $-0.65$  V. Although not evident on this absorbance scale, spectrum (a) is the same as the original spectrum of  $\text{Cu}(\text{en})_2^{2+}$ . Starting at  $-0.65$  V and continuing to  $-0.9$  V the spectrum of  $\text{Cu}(\text{nc})_2^{1+}$  with  $\lambda_{\text{max}} = 454$  nm grows in (spectra 3b–3c), confirming the formation of  $\text{Cu}(\text{nc})_2^{1+}$  as the reduction product of  $\text{Cu}(\text{en})_2^{2+}$  under these conditions. Scanning to more negative potentials leads to hydrogen evolution. Holding the potential at  $-0.9$  V for 15 min gives an additional large increase in absorbance at 454 nm (3c–3d), which then stops. The baseline did not change, thus indicating that no copper deposits on ITO OTE. If the potential is scanned back from  $-0.9$  V to 0.8 V (3d–3e), considerable time is required for  $\text{Cu}(\text{nc})_2^{1+}$  to be oxidized and exchange nc for en to reform  $\text{Cu}(\text{en})_2^{2+}$ . The potential must be held at 0.8 V for 30 min before the original spectrum is finally obtained (3e–3a). Thus, the thin-layer spectroelectrochemistry shows quantitative cycling between  $\text{Cu}(\text{en})_2^{2+}$  and  $\text{Cu}(\text{nc})_2^{1+}$ , albeit with a large potential separation and a very slow rate.

Repeating this experiment in the absence of nc gave no change in absorbance when the potential was scanned from 0.8 V to  $-0.8$  V. However, there was an increase in absorbance at all wavelengths when the potential was scanned

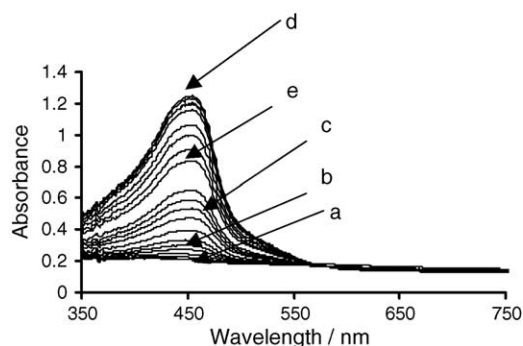


Fig. 3. Absorbance spectra of a 7.5 mM  $\text{CuSO}_4$  solution made with  $2 \times 10^{-2}$  M en,  $2 \times 10^{-2}$  M nc, and 0.1 M  $\text{KNO}_3$  in 1:3 (v/v) ethanol in water taken during the reduction process in an ITO OTTLE in the potential range from 0.8 V to  $-0.9$  V (vs. Ag/AgCl ref) at 5 mV/s. (a) Cycling the potential from 0.8 V to  $-0.65$  V at 5 mV/s, (b–c) scanning the potential from  $-0.65$  V to  $-0.9$  V, (c–d) scanning the potential from  $-0.9$  V to 0.8 V, (e–a) The potential was held at 1.0 V for 30 min.

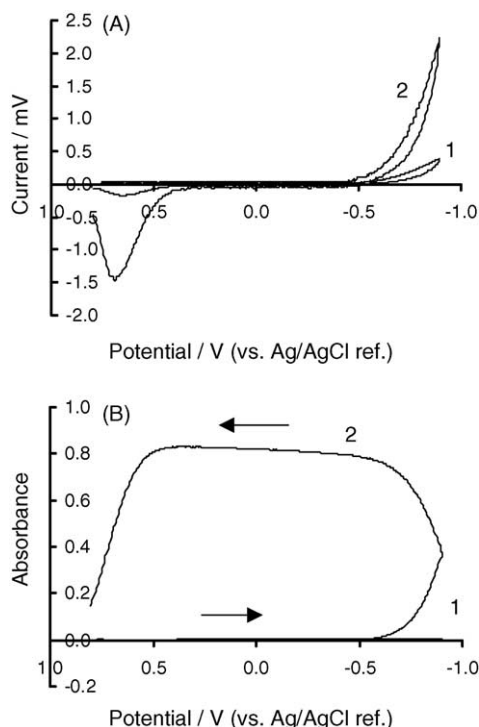


Fig. 4. Enhancement of the electrochemical and optical signals by the presence of Nafion-SiO<sub>2</sub>. (A) Cyclic voltammograms of a bare OTE (curve 1) and an OTE modified with Nafion-SiO<sub>2</sub> (curve 2). (B) Sensor absorbance vs. time responses corresponding to voltammograms in A. The measurements were begun at 20 min post injection of  $1 \times 10^{-3}$  M CuSO<sub>4</sub> solution with  $4 \times 10^{-3}$  M en in 0.1 M KNO<sub>3</sub>. The potential was scanned from 0.8 V to  $-0.9$  V (5 mV/s, vs. Ag/AgCl ref.).

from  $-0.8$  V to  $-0.9$  V due to deposition of Cu<sup>0</sup> at the electrode surface (not shown).

Cyclic voltammograms of Cu(en)<sub>2</sub><sup>2+</sup> at a Nafion-SiO<sub>2</sub> ITO OTE with trapped nc and at a bare ITO OTE with an excess of nc in solution are shown in Fig. 4A. The voltammograms are very similar except that the peak current is three times larger at the modified electrode than at the bare ITO electrode due to pre-concentration of Cu(en)<sub>2</sub><sup>2+</sup> into the

Nafion-SiO<sub>2</sub> film. Noteworthy is the absence of a Cu<sub>2</sub>O stripping peak in either case.

Fig. 4B shows the corresponding ATR optical signals recorded concurrently with the voltammograms in Fig. 4A. At the Nafion-SiO<sub>2</sub> ITO OTE the absorbance at 454 nm increases substantially at potentials negative of  $-0.5$  V, which is consistent with formation of Cu(nc)<sub>2</sub><sup>1+</sup>. The absorbance decreases when the potential exceeds 0.5 V on the reverse scan. At the end of the positive scan (0.2 V), the absorbance is about 0.18 AU; however, it decreases back to its original value of 0 AU if the potential is held at this value for about 10 min.

Comparison of the response at the modified electrode versus the bare electrode (barely visible in Fig. 4b) shows a change in absorbance that is 250 times larger at the modified electrode. Large sensitivity enhancement was provided by pre-concentration into the Nafion-SiO<sub>2</sub> coated ITO OTE.

### 3.3. Effect of nc concentration in the Nafion film

The effect of the concentration of nc in the film was studied by varying the concentration of nc in the contact solution during the loading process and then by exposing the nc-loaded film to a solution of 1.0 mM Cu(en)<sub>2</sub><sup>2+</sup>. The film was exposed to each nc solution for 3 h during loading. The concentration of nc in the contact solution was varied from  $4.0 \times 10^{-4}$  M to  $4.0 \times 10^{-2}$  M, yielding a concentration of nc in the film varying from  $5 \times 10^{-3}$  M to 0.84 M. The concentration of nc in the film was estimated by measuring an absorbance difference ( $\Delta A = A_{(\text{nc in solution before uptake})} - A_{(\text{nc in solution after uptake})}$ ) from 4.1 mL of nc solution in a cuvette and substituting this into Beer's Law ( $\Delta A = \epsilon bc$ ) using  $\epsilon_{(\text{nc at } 300 \text{ nm})} = 8695 \text{ M}^{-1} \text{ cm}^{-1}$ . A summary of these experiments is provided in Table 2. For a constant Cu(en)<sub>2</sub><sup>2+</sup> concentration in sample solution,  $\Delta A$  increases with increasing nc in the film until nc in the film exceeds Cu(en)<sub>2</sub><sup>2+</sup> by about a factor of two. This is the ratio that would stoichiometrically convert all Cu(en)<sub>2</sub><sup>2+</sup> to Cu(nc)<sub>2</sub><sup>1+</sup>. Higher concentrations of nc gave

Table 2  
Effect of ligand concentration in the film

| nc concentration in contact solution, (M) <sup>a</sup> | nc concentration in the film, (M) <sup>b</sup> | $\Delta A$ <sup>c</sup> | Concentration of Cu(en) <sub>2</sub> <sup>2+</sup> in the film <sup>d</sup> | [nc]/[Cu] ratio in the film <sup>e</sup> |
|--|--|-------------------------|---|--|
| $4.0 \times 10^{-4}$                                   | 0.005  | 0.006                   | 0.002   | 2.5:1                                    |
| $4.0 \times 10^{-3}$                                   | 0.18   | 0.30                    | 0.10  | 1.8:1                                    |
| $1.0 \times 10^{-2}$                                   | 0.39   | 0.60                    | 0.20  | 2.0:1                                    |
| $2.0 \times 10^{-2}$                                   | 0.64   | 0.83                    | 0.29  | 2.2:1                                    |
| $3.0 \times 10^{-2}$                                   | 0.84   | 0.60                    | 0.20  | 4.2:1                                    |
| $4.0 \times 10^{-2}$                                   | 0.84   | 0.53                    | 0.18  | 4.7:1                                    |

<sup>a</sup> Concentration of nc used for pre-concentration ( $t = 4$  h).

<sup>b</sup> Estimate of concentration of nc in the film (as estimated by  $\Delta A = A_{(\text{nc solution before uptake})} - A_{(\text{nc solution after uptake})}$ , and volume of the cell 4.1 mL, and  $\epsilon_{(\text{nc at } 300 \text{ nm})} = 8695 \text{ cm}^{-1} \text{ M}^{-1}$ , where  $A = \epsilon bc$ ).

<sup>c</sup>  $\Delta A$  is the change in absorbance of Cu(en)<sub>2</sub><sup>2+</sup> pre-concentrated from 1 mM solution and nc in the film.

<sup>d</sup> Estimate of concentration of Cu(en)<sub>2</sub><sup>2+</sup> in the film (as estimated by penetration depth and 10 reflections, and  $\epsilon_{(\text{Cu}(\text{en})_2^{2+})} = 7950 \text{ cm}^{-1} \text{ M}^{-1}$ , where  $\Delta A = \epsilon bc$ ).

<sup>e</sup> Ratio of estimated nc concentration to estimated Cu(en)<sub>2</sub><sup>2+</sup> concentration in the film.

no further increase in  $\Delta A$ , but rather caused a decrease in signal. The reason for this behavior is not known, but perhaps a high concentration of nc in the film makes the film more hydrophobic, causing a decrease in partitioning of hydrophilic  $\text{Cu}(\text{en})_2^{2+}$ . The optimal performance of the sensor was achieved with the concentration of nc in the film equal to 0.64 M. Here, the sensor shows the highest change in absorbance,  $\Delta A = 0.83$ , for 1 mM  $\text{Cu}(\text{en})_2^{2+}$  solution (Table 2). Thus, the detection limit of  $\text{Cu}(\text{en})_2^{2+}$  should be optimized under these conditions. However, we note that the range of the calibration curve is limited on the upper end by the concentration of nc in the film.

### 3.4. Effect of scan rate on modulated absorbance

The rate of potential scanning during spectroelectrochemical modulation has a large effect on the absorbance versus time profile as illustrated in Fig. 5 for a  $\text{Cu}(\text{en})_2^{2+}$  loaded nc-Nafion-SiO<sub>2</sub> film. At the slowest scan rate investigated (1 mV/s), complete conversion of  $\text{Cu}(\text{en})_2^{2+}$  to  $\text{Cu}(\text{nc})_2^{1+}$  during the reduction cycle is evidenced by plateauing of the absorbance at ca. 0.75 AU. However, conversion back to  $\text{Cu}(\text{en})_2^{2+}$  is incomplete as evidenced by plateauing at 0.15 AU on the oxidation cycle, rather than returning to 0 AU. We attribute this behavior primarily to the slow kinetics of the ligand exchange reaction to regenerate  $\text{Cu}(\text{en})_2^{2+}$ . Even though conversion is incomplete, the signal levels off because the potential begins its second cycle in which it becomes too negative to oxidize  $\text{Cu}(\text{nc})_2^{1+}$ . This situation is made worse by faster scan rates for which  $\Delta A$  systematically decreases with increasing scan rate. Increasing the potential scan rate also causes the electrochemical diffusion layer thickness to become thinner than the sensing film and the penetration depth of the evanescent beam (i.e., the optical path). This in turn leads to incomplete electrolysis in the film for conversion of  $\text{Cu}(\text{en})_2^{2+}$  to  $\text{Cu}(\text{nc})_2^{1+}$  in Nafion-SiO<sub>2</sub>. Full conversion was estimated by reducing  $\text{Cu}(\text{en})_2^{2+}$  chemically by adding excess hydroxylamine to the solution and waiting for 30 min for ligand exchange to occur with the excess of nc in the film. At 1 mV/s 100% conversion was achieved

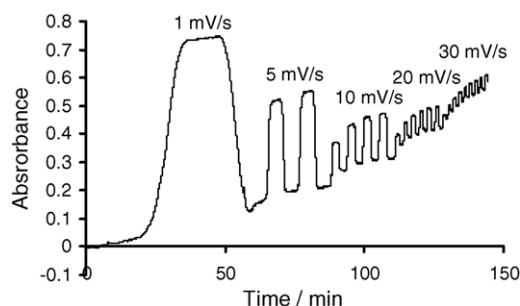


Fig. 5. Modulation at 450 nm for  $\text{CuSO}_4$  taken up into a Nafion-SiO<sub>2</sub> thin film coated on ITO-glass at steady-state film loading in nc and in  $5.0 \times 10^{-4}$  M  $\text{CuSO}_4$  and  $4 \times 10^{-3}$  M en. (0.1 M  $\text{KNO}_3$  supporting electrolyte). The potential was scanned between 0.8 and  $-0.9$  V (triangular wave) at 1, 5, 10, 20, 30 mV/s scan rates.

based on comparison to the data obtained using the chemical reducing agent. Since conversion decreases as the potential scan rate increases, very slow electromodulation is required if maximum  $\Delta A$  is desired.

### 3.5. Calibration curve

A representative calibration curve for standard solutions of  $\text{Cu}(\text{en})_2^{2+}$  is shown in Fig. 6. Fig. 6A illustrates the optical response driven by the electrochemical reduction and ligand exchange converting  $\text{Cu}(\text{en})_2^{2+}$  to  $\text{Cu}(\text{nc})_2^{1+}$  as the potential was scanned between 0.8 V and  $-0.9$  V at 5 mV/s.

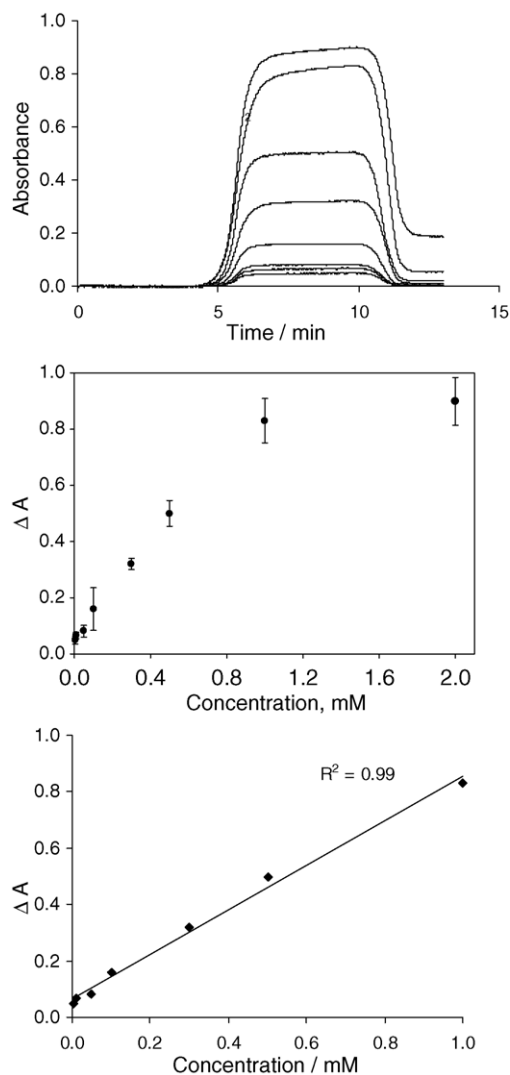


Fig. 6. Calibration data for  $\text{Cu}(\text{en})_2^{2+}$  taken up into a Nafion-SiO<sub>2</sub>-nc film. (A) The ATR optical responses driven by the electrochemical and chemical changes of  $\text{Cu}(\text{en})_2^{2+}$  to  $\text{Cu}(\text{nc})_2^{1+}$  for (1)  $5 \times 10^{-6}$  M, (2)  $1 \times 10^{-5}$  M, (3)  $5 \times 10^{-5}$  M, (4)  $1 \times 10^{-4}$  M, (5)  $3 \times 10^{-4}$  M, (6)  $5 \times 10^{-4}$  M, (7)  $1 \times 10^{-3}$  M, and (8)  $2 \times 10^{-3}$  M  $\text{CuSO}_4$  with  $4 \times 10^{-3}$  en. (B) Calibration plot of  $\Delta A$  vs. concentration. (C) The linear range of the calibration plot. All measurements were taken at 450 nm after the film was equilibrated with  $\text{CuSO}_4$  solutions containing  $4 \times 10^{-3}$  M en and 0.1 M  $\text{KNO}_3$  supporting electrolyte. The potential was scanned between 0.8 V and  $-0.9$  V at 5 mV/s.

These optical responses ( $\Delta A$ ) were used to generate the calibration curves in Fig. 6B and C. Fig. 6B shows the curve over a broad range of concentrations, whereas Fig. 6C is restricted to the linear region. The curve has a limited linear range spanning  $\text{Cu}(\text{en})_2^{2+}$  concentrations of  $5 \times 10^{-6}$  M to  $1 \times 10^{-3}$  M and deviates negatively at higher concentrations. The non-linearity at higher concentrations is due to one or more factors that could include: (1) non-linear partitioning of  $\text{Cu}(\text{en})_2^{2+}$  into the film as it becomes saturated; (2) insufficient excess of nc in the film for stoichiometric ligand exchange; and (3) slow ligand exchange if the potential scan rate is too fast. The error bars in Fig. 6B represent the reproducibility achieved at each concentration with three different electrodes. These deviations are due to differences in the ITO electrodes, differences in film thickness and composition, and distribution of nc and ion-exchange sites within the film. The optimal nc concentration in the contact solution as determined above was used for the ligand uptake. Though the conversion at 5 mV/s is only 48% complete, this scan rate was used to generate the calibration curve in order to speed up the analysis time; we note that scanning at 1 mV/s should lead to lower limits of detection.

The sensing film can be used multiple times provided it is washed thoroughly with 0.5 M potassium nitrate after each use in order to remove partitioned analyte.

#### 4. Conclusions

The concept of ligand exchange within the sensing film as a means of significantly enhancing the sensitivity for detection of a metal complex ion by spectroelectrochemistry has been demonstrated.  $\text{Cu}(\text{en})_2^{2+}$  and nc serve as a good, but not ideal, system for this demonstration. The major disadvantage of the system is the slow rate of ligand exchange, which contributed to slow sensor response.

An important aspect of the sensor is the Nafion-SiO<sub>2</sub> film, which served the dual role of pre-concentrating  $\text{Cu}(\text{en})_2^{2+}$  in the optical path of the sensor and storing nc for the ligand exchange reaction. The dual nature of Nafion enabled it to both pre-concentrate hydrophilic  $\text{Cu}(\text{en})_2^{2+}$  by cation exchange with its anionic sulfonate groups and to load hydrophobic nc through interaction with the hydrophobic domains.

A calibration curve for  $\text{Cu}(\text{en})_2^{2+}$  is linear from  $5 \times 10^{-6}$  M to  $1 \times 10^{-3}$  M with a detection limit of  $1 \times 10^{-6}$  M. These performance factors should be regarded as specific to the cell and the procedure used in this work. At the lower concentrations, a substantial fraction of the analyte is removed from the sample, which ultimately restricts the detection limit. Substantially lower limits of detection can be obtained by circulating a large volume of sample through the cell so that partitioning into the film has a negligible effect on the bulk sample concentration.

Neocuproine was chosen as a ligand because it forms a very stable, strongly absorbing complex with  $\text{Cu}^{1+}$ . Neocuproine also forms complexes with other metal ions

such as  $\text{Co}^{2+}$ ,  $\text{Ni}^{2+}$ ,  $\text{Zn}^{2+}$ , and  $\text{Cd}^{2+}$ . The selectivity of the sensor for  $\text{Cu}(\text{en})_2^{2+}$  in the presence of such interferences will depend on stability constants, electrochemical characteristics, and spectral properties of the interfering species. For this particular list of metal ions, the stability constants of their complexes with nc are much smaller than for  $\text{Cu}^+$  (7.0, 8.5, 7.7, 10.4, respectively) [21] and the spectroelectrochemical properties of these complexes are also very different. Therefore, nc is an excellent choice of ligand for the selective determination of copper complexes. However, future work on this sensor should include a careful evaluation of possible interferences by these and other metal ions such as antimony, which interferes with the determination of copper by stripping voltammetry.

The ligand exchange mechanism for enhancing  $\Delta \varepsilon$  as demonstrated herein is a general strategy that should be extendable to other metal ions by judicious choice of appropriate ligands and charge-selective films.

#### Acknowledgments

This work was supported by a grant awarded by the Environmental Management Science Program of the U.S. Department of Energy, Office of Environmental Management (DE-FG07-99ER62311-70010 and a University of Cincinnati Doctoral Investment Award).

#### References

- [1] Y. Shi, A.F. Slaterbeck, S. Aryal, C.J. Seliskar, W.R. Heineman, T.H. Ridgway, J.H. Nevin, *Proc. SPIE* 3258 (1998) 56.
- [2] Y. Shi, A.F. Slaterbeck, C.J. Seliskar, W.R. Heineman, *Anal. Chem.* 69 (1997) 3679.
- [3] Y. Shi, C.J. Seliskar, W.R. Heineman, *Anal. Chem.* 69 (1997) 4819.
- [4] A.F. Slaterbeck, T.H. Ridgway, C.J. Seliskar, W.R. Heineman, *Anal. Chem.* 71 (1999) 1196.
- [5] L. Gao, C.J. Seliskar, W.R. Heineman, *Anal. Chem.* 71 (1999) 4061.
- [6] L. Gao, C.J. Seliskar, W.R. Heineman, *Electroanalysis* 13 (2001) 613.
- [7] Z. Hu, C.J. Seliskar, W.R. Heineman, *Anal. Chem.* 70 (1998) 5230.
- [8] Z. Hu, A.F. Slaterbeck, C.J. Seliskar, T.H. Ridgway, W.R. Heineman, *Langmuir* 15 (1999) 767.
- [9] A.F. Slaterbeck, M.L. Stegemiller, C.J. Seliskar, T.H. Ridgway, W.R. Heineman, *Anal. Chem.* 72 (2000) 5567.
- [10] M.L. Stegemiller, W.R. Heineman, T.H. Ridgway, C.J. Seliskar, S.A. Bryan, T. Hubler, *Anal. Chem.* 73 (2001) 3420.
- [11] J.M. DiVirgilio-Thomas, W.R. Heineman, C.J. Seliskar, *Anal. Chem.* 72 (2000) 3461.
- [12] M. Clager, C.J. Seliskar, W.R. Heineman, Unpublished results.
- [13] L. Gao, C.J. Seliskar, L. Milstein, *Appl. Spectrosc.* 51 (1997) 1745.
- [14] M. Maizels, M.L. Stegemiller, S.E. Ross, A.F. Slaterbeck, Y. Shi, T.H. Ridgway, W.R. Heineman, C.J. Seliskar, S.A. Bryan, in: P.G. Eller, W.R. Heineman (Eds.), *ACS Symposium Series 778: First Accomplishments of the Environmental Science Program*, American Chemical Society, Washington, DC, 2001, p. 364.
- [15] Y. Shi, C.J. Seliskar, *Chem. Mater.* 9 (1997) 821.
- [16] L. Gao, C.J. Seliskar, *Chem. Mater.* 10 (1998) 2481.
- [17] J.N. Richardson, A.L. Dyer, M.L. Stegemiller, I. Zudans, C.J. Seliskar, W.R. Heineman, *Anal. Chem.* 74 (2002) 3330.

- [18] C. Piraud, E. Mwarania, G. Wylangowski, J. Wilkinson, K. O'Dwyer, D.J. Schiffrin, *Anal. Chem.* 64 (1992) 651.
- [19] T.P. DeAngelis, W.R. Heineman, *J. Chem. Ed.* 53 (1976) 594.
- [20] M. Scholten, J.E.A.M. van der Meerakker, *J. Electrochem. Soc.* 140 (1993) 471.
- [21] R.M. Smith, A.E. Martell, *Critical Stability Constants*, Plenum Press, New York, 1975.
- [22] G.F. Smith, W.H. McCurdy, *Anal. Chem.* 24 (1952) 371.
- [23] Y. Yamini, A. Tomaddon, *Talanta* 49 (1999) 119.
- [24] J.R. Tuschall, P.L. Brezonik, *Anal. Chem.* 53 (1981) 1986.
- [25] J.M. Diaz-Cruz, C. Arino, M. Esteban, E. Casassas, *Electroanalysis* 5 (1993) 677.
- [26] I.M. Kolthoff, J.J. Lingane, *Polarography*, Interscience, New York, 1952.
- [27] M.L.S. Simoes-Soncalves, L. Sigg, *Electroanalysis* 3 (1991) 553.
- [28] Y. Shacham-Diamond, *Thin Solid Films* 262 (1995) 93.
- [29] K.C. Honeychurch, J.P. Hart, D.C. Cowell, *Electroanalysis* 12 (2000) 171.
- [30] T. Shtoyko, S. Conklin, A.T. Maghasi, J.N. Richardson, A. Piruska, C.J. Seliskar, W.R. Heineman, *Anal. Chem.* 76 (2004) 1466.